A TRIDENT SCHOLAR PROJECT REPORT

NO. 529

Enhancement of Metal-Organic Framework Systems for Degradation of Nerve Agents

by

Midshipman 1/C William T. Ashe, USN

UNITED STATES NAVAL ACADEMY
ANNAPOLIS, MARYLAND

USNA-1531-2

REPORT DOCUMENTATION PAGE

Form Approved
OMB No. 0704-0188

1. REPORT DATE *(DD-MM-YYYY)*	**2. REPORT TYPE**	**3. DATES COVERED** *(From - To)*
5-16-23		

4. TITLE AND SUBTITLE
Enhancement of Metal-Organic Framework Systems for Degradation of Nerve Agents

5a. CONTRACT NUMBER

5b. GRANT NUMBER

5c. PROGRAM ELEMENT NUMBER

6. AUTHOR(S)
William T. Ashe

5d. PROJECT NUMBER

5e. TASK NUMBER

5f. WORK UNIT NUMBER

7. PERFORMING ORGANIZATION NAME(S) AND ADDRESS(ES)

8. PERFORMING ORGANIZATION REPORT NUMBER

9. SPONSORING / MONITORING AGENCY NAME(S) AND ADDRESS(ES)
U.S. Naval Academy
Annapolis, MD 21402

10. SPONSOR/MONITOR'S ACRONYM(S)

11. SPONSOR/MONITOR'S REPORT NUMBER(S)
Trident Scholar Report no. 529 (2023)

12. DISTRIBUTION / AVAILABILITY STATEMENT

This document has been approved for public release; its distribution is UNLIMITED.

13. SUPPLEMENTARY NOTES

14. ABSTRACT

Metal-organic frameworks (MOFs) show potential as Lewis acid catalysts for the destruction of organophosphate nerve agents. Previously, they required a volatile aqueous base to achieve ideal degradation reaction kinetics. Recent success has been achieved in incorporating azole bases into MOFs that enhance the catalytic degradation of organophosphate nerve agent mimic. This project encapsulated azole derivatives into zirconium-based MOF structures to yield MOF composites. Nuclear magnetic resonance (NMR) spectroscopy, thermogravimetric analysis, and physisorption experiments confirmed each MOF's structure and physical properties. The reaction kinetics of each MOF were evaluated via hydrolysis of DMNP, a nerve agent mimic, using 31P NMR; these data reveal that MOF composites containing imidazole and 3-amino-1,2,4-triazole increased reaction rates >250% compared to controls. MOF was then immobilized within a mesoporous natural fiber welded (M-NFW) cellulose fabric. The kinetics of DMNP degradation by these MOF-fabrics was monitored using UV-Vis spectroscopy. MOF composites that do not require volatile base to carry out catalyzed hydrolysis of organophosphate nerve agents provide a time-effective approach to combating nerve agents. Integrating these nanomaterials into M-NFW cellulose fabric is a novel way to implement MOF structures for applications such as gas mask filters and clothing that protect personnel during chemical warfare attacks.

15. SUBJECT TERMS
Metal-Organic Framework, Degradation, Nerve Agent, Cellulose, Natural Fiber Welding

16. SECURITY CLASSIFICATION OF:			**17. LIMITATION OF ABSTRACT**	**18. NUMBER OF PAGES**	**19a. NAME OF RESPONSIBLE PERSON**
a. REPORT	**b. ABSTRACT**	**c. THIS PAGE**		34	**19b. TELEPHONE NUMBER** *(include area code)*

U.S.N.A. --- Trident Scholar project report; no. 529 (2023)

Enhancement of Metal-Organic Framework Systems for Degradation of Nerve Agents

by

Midshipman 1/C William T. Ashe
United States Naval Academy
Annapolis, Maryland

_____
(signature)

Certification of Adviser(s) Approval

Professor Craig M. Whitaker
Chemistry Department

_____
(signature)

_____
(date)

CDR David P. Durkin, USN
Chemistry Department

_____
(signature)

_____
(date)

Acceptance for the Trident Scholar Committee

Professor Maria J. Schroeder
Associate Director of Midshipman Research

_____
(signature)

_____
(date)

USNA-1531-2

Abstract

Metal-organic frameworks (MOFs) show great potential as Lewis acid catalysts for the destruction of organophosphate nerve agents such as sarin gas. Previously, they required a separate volatile aqueous base to achieve results that demonstrated ideal degradation reaction kinetics. Recent success has been achieved in incorporating azole bases into MOFs that enhance the catalytic degradation of organophosphate nerve agent mimic. This project details the effects of encapsulating azole derivatives, namely imidazole and triazoles, into zirconium-based MOF structures to yield MOF composites. Four mesoporous MOFs with average pore diameter of 2 - >10 nm were synthesized and studied. Nuclear magnetic resonance (NMR) spectroscopy, thermogravimetric analysis (TGA) and physisorption experiments confirmed each MOF's structure and physical properties. The reaction kinetics of each MOF were evaluated via hydrolysis of dimethyl *p*-nitrophenyl phosphate (DMNP), a nerve agent mimic of sarin, using ^{31}P NMR; these data reveal that MOF composites containing imidazole and 3-amino-1,2,4-triazole increased reaction rates >250% compared to controls. These reaction rates approached the fastest degradation rates reported in the literature, without the use of a volatile aqueous base. Each baseline MOF was then immobilized within a mesoporous natural fiber welded cellulose fabric. The kinetics of successful DMNP degradation by these MOF-fabrics was monitored utilizing a UV-Vis spectroscopy method developed in-house. The discovery of new MOF composites that do not require constant replenishment of base to carry out catalyzed hydrolysis of organophosphate nerve agents provides a realistic and time-effective approach to combating chemical warfare in both arid and humid environments. Integrating these nanomaterials into mesoporous natural fiber welded cellulose fabric is a novel and effective way to implement MOF structures for many Department of Defense and civilian applications, including gas mask filters and clothing that protect personnel during chemical warfare attacks.

Keywords: Metal-Organic Framework, Degradation, Nerve Agent, Cellulose, Natural Fiber Welding

Acknowledgements

This project was largely derived from the 2021 work of H. Luo, A. Castro, M. Wasson, W. Flores, O. Farha, and Y. Liu at California State University and Northwestern University. Thank you to Craig Whitaker, Ph.D. for his guidance throughout the years of work in his lab. Thank you to Gregory Peterson, Ph.D. for the collaboration with CCBC Chemical and Biological Center. Thank you to CDR David Durkin, USN for the help with physisorption measurements and thermogravimetric analysis as well as developing the materials these MOFs were eventually incorporated into along with Paul Trulove, Ph.D., Nathaniel Larm, Ph.D., and fellow Trident Scholar Midshipman Anders Gulbrandson. This work was supported by Trident awards and Midshipmen Research Support (MRS) grants.

Table of Contents

I. Introduction

Organophosphate compounds are used in pesticides, Alzheimer's medication, and notably chemical warfare.[1] Since their synthesis in the 1930's, organophosphate nerve agents have terrorized the battlefield and civilian communities. Recently, they have been used against the Kurdish people of Northern Iraq during the Iraq-Iran war (1980-1988), as well as Japanese (1995) and Syrian (2013) civilians.[2] The search for an efficient method to protect individuals from the harmful effects of nerve agents is ongoing. One promising pathway is to use metal-organic frameworks (MOFs) due to their structural adaptability and porous nature. This allows for a fine-tuned microenvironment in which the degradation of the nerve agent can occur. Many different types of MOFs have proven capable of reacting with organophosphate nerve agents, however a consistent consideration that must be addressed is their relatively slow rate of kinetics for nerve agent degradation.

MOF systems are composed of inorganic clusters of atoms connected by organic linkers that form a repeating, porous crystalline structure, as shown in Figure 1 from Venturi et al.[3] Altering the organic linkers and metals used in a MOF tunes pore size and catalyzes specific chemical reactions. MOFs have been used for catalysis, gas storage/capture, drug delivery, and other applications.[4] For this study, the reaction of interest is the catalyzed hydrolysis of organophosphate nerve agents. Specifically, zirconium-based frameworks will be used due to their past success in hydrolysis reactions. MOFs that have had positive results typically contain micro- and mesopores with 1.3-3.4 nm diameters.[5] The hydrolysis is catalyzed by the inorganic zirconium nodes, which serve as a Lewis acid catalyst.[6] It is important that the MOF's pores are wide enough to encapsulate the organophosphate compounds while keeping proximity to an inorganic node.

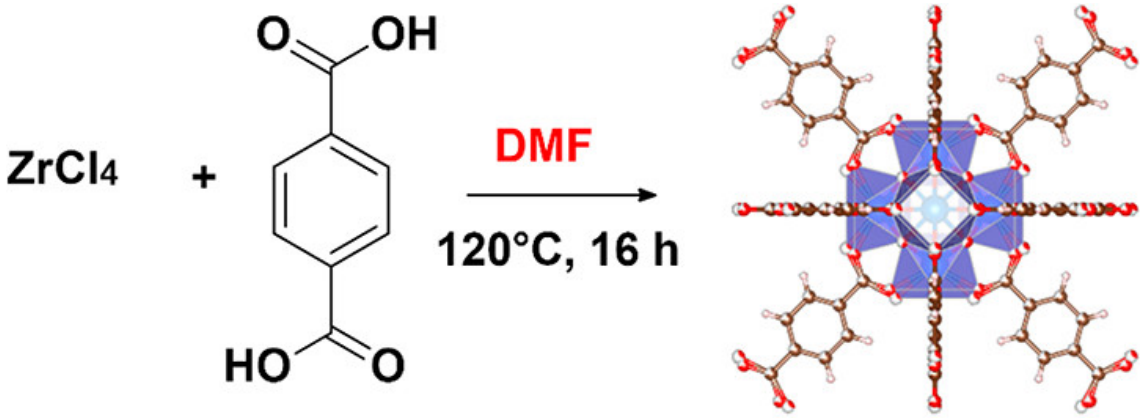

Figure 1. Synthesis of zirconium-based MOF UiO-66. The overall framework is shown on the right and is a series of inorganic clusters connected by organic linkers.

These MOF systems lower the activation energy required to degrade nerve agents to a less toxic form. However, a volatile liquid base must typically be added to an aqueous buffer to allow the reaction to occur.[7] This is not practical for actual applications because chemical warfare attacks are likely to occur in ambient environmental conditions. Therefore, it is necessary to develop MOF systems capable of hydrolyzing nerve agents under real world conditions.

Developing a MOF capable of hydrolyzing nerve agents at an acceptable rate is only part of the solution. Additionally, it is necessary to incorporate these MOFs into a usable material for gas mask filters, clothing, and other applications. MOFs have been successfully integrated into different types of fabrics using a variety of methods, including *in-situ* growth of MOFs onto fabrics and vapor-sorption synthesis.[8] Recently, a new approach to MOF-fabric integration using a high surface area cellulose matrix to trap nanoparticles (NP) has been reported.[9] The process of Natural Fiber Welding (NFW) has recently been developed to create high surface area fabrics that can contain nanomaterials such as MOFs, while retaining the preferred properties of the underlying material.[10, 11] Upon trapping of the MOFs, the MOF-fabric complex can facilitate the hydrolysis of organophosphate nerve agents.

II. Background

a. Organophosphate Nerve Agent Mechanism of Action

Chemical warfare agents take many different forms, but some of the most lethal are organophosphate nerve agents. These consist of a phosphoric acid derivative with four different functional groups on the phosphorus. The different functional groups contribute to adjustable physical properties and chemical makeups that can be adapted for specific purposes. For example, one nerve agent called VX is lipophilic (dissolvable in lipids or fat) and can be absorbed through the skin easily. Its low volatility (10 mg m^{-3} at 25°C) allows it to remain in its environment for longer than more volatile nerve agents such as sarin (volatility at 25°C is 22,000 mg m^{-3}).[12]

After entering the body, these nerve agents can attack the nervous system by disrupting the process of muscle contractions. In the nervous system, the molecule acetylcholine binds to receptors on muscle cells which allow for transmission of nerve impulses between synapses. While acetylcholine is critical for life functions such as muscle contractions, it must be digested for muscles to relax. After a nerve impulse transmission, the enzyme acetylcholinesterase (AChE) hydrolyzes acetylcholine (see Figure 2). AChE has a high catalytic efficiency (i.e., ~10^8) which is irreversibly inhibited by nerve agents, causing the host to have sustained stimulation of the muscle cells that can lead to death.[12]

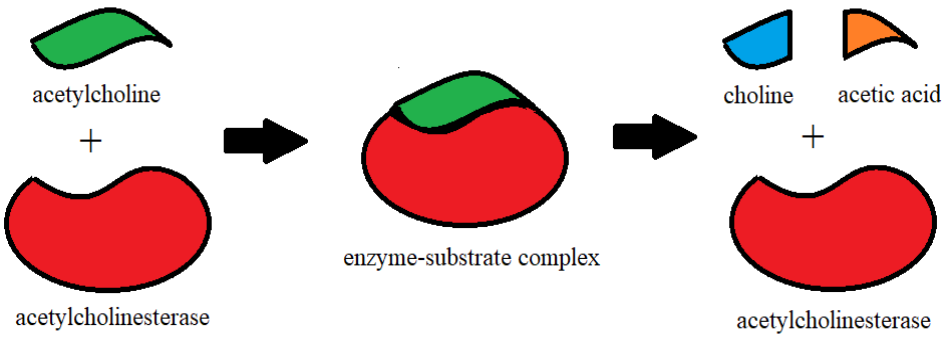

Figure 2. A model of the mechanism of acetylcholine interacting with acetylcholinesterase.

Organophosphate nerve agents are highly toxic and too dangerous to work with under typical laboratory conditions. Fortunately, simulants that closely resemble the structure of the actual nerve agents, but are less toxic, can be used in a normal laboratory setting with proper hood ventilation. The simulant used in this study is dimethyl *p*-nitrophenyl phosphate (DMNP), which structurally resembles sarin gas as shown in Figure 3. Functionally, it degrades in a similar mechanism to sarin and can more safely provide insight into how an actual nerve agent would behave under experimental conditions.

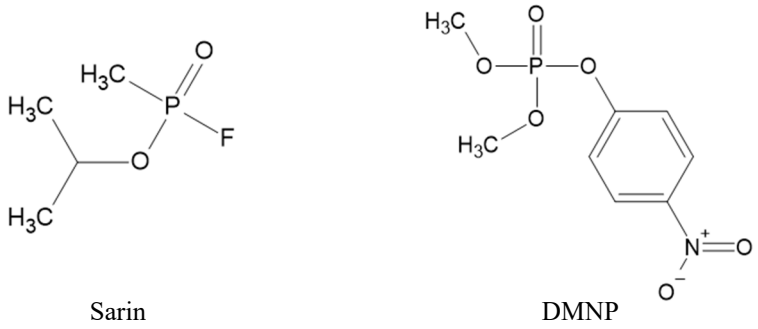

Figure 3. Sarin and DMNP structures.

b. Metal-Organic Framework Structure and Function

MOFs are a novel class of macromolecules that link organic and inorganic structures together to form a scalable and adaptable medium capable of performing a variety of functions. These porous systems consist of metal-based inorganic nodes connected by organic linkers in a repeating pattern with predictable pore size. Figure 4 from Lawrence et al. shows the MOF UiO-67, which consists of a single octahedral cage with smaller tetrahedral cages on its faces.[13] UiO-67's inorganic sections are composed of cationic $Zr_6O_4(OH)_4$ nodes and its linkers are formed using biphenyl-4,4'-dicarboxylate. By changing the nature of the nodes and linkers, this approach can form thousands of unique MOF structures. This study will focus on the family of zirconium-based MOFs, due to their ability to degrade nerve agents.[5-7]

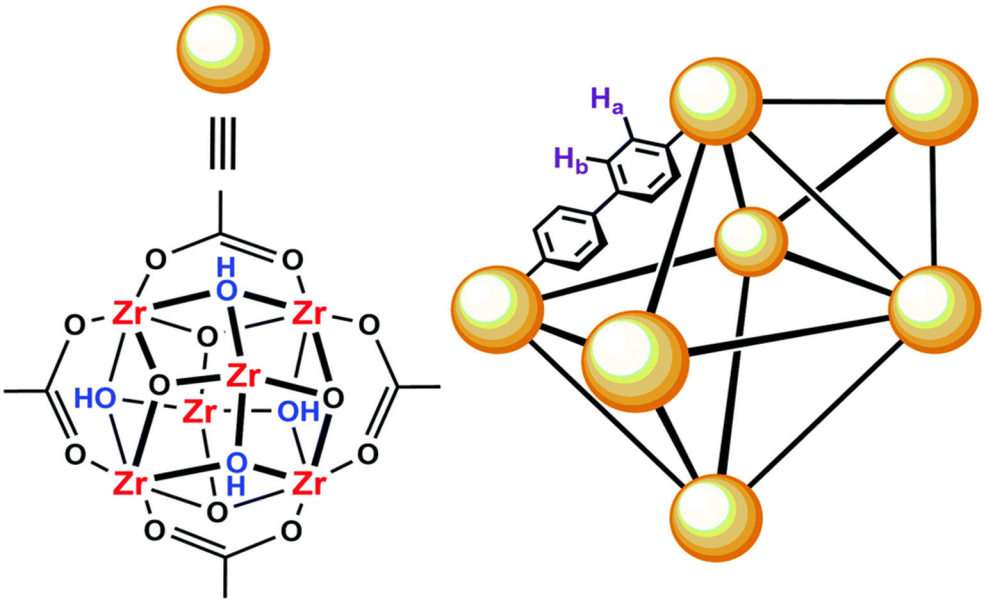

Figure 4. Subunit of UiO-67 MOF and its organic linker biphenyl-4,4'-dicarboxylate.

New functions for MOFs have recently been discovered including energy storage, gas separation, and the catalytic decomposition of toxic nerve agents as seen in this study.[4] MOFs have a variety of different functions due to their high surface area and tunable pore sizes. These pores can be the site of various chemical reactions, as seen in this study, or storage vessels for gases and other compounds. In this case, the MOF pore size is tuned to allow for optimized organophosphate nerve agent entry and proximity to the inorganic nodes. One desirable aspect of MOFs is their ability to covalently bond a species to the organic linker, or to encapsulate a molecule into the framework's pores to perform a specific function.

c. Natural Fiber Welding

The process of Natural Fiber Welding (NFW) is a patented biopolymer engineering process discovered around 2010 at the United States Naval Academy by Haverhals, et al.[14-16] In this process, ionic liquids (IL) are applied to the surface of a biopolymer such as cellulose. This causes the surface of the material to swell and solubilize, which allows the fiber strands to interact with one another. The sample is then exposed to heat and the IL is washed off using a solvent. A congealed network of biopolymer fiber is left behind that retains much of its native structure, but results in composites with improved physical properties (i.e., strength and toughness). By utilizing different treatment times and temperatures, the biopolymer can be altered to different degrees depending on the properties desired. Native biopolymers and their welded counterparts can be seen in Figure 5 from Haverhals et al.[16]

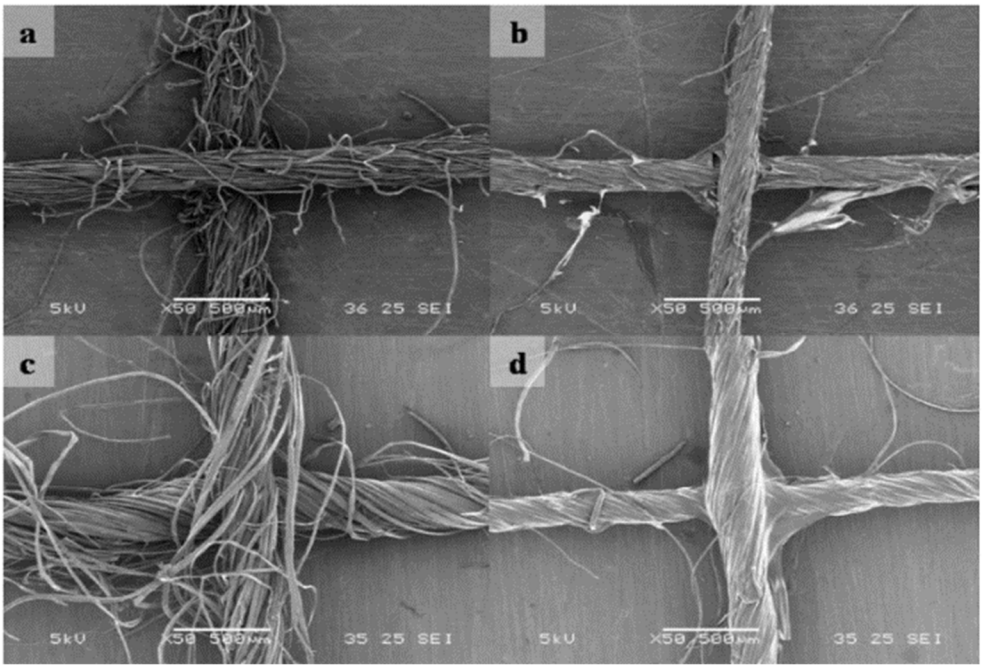

Figure 5. Examples of fiber welding cotton and hemp. Figure panel designations are as follows: (a) cotton thread, (b) cotton thread treated for 5 min at 60°C, (c) hemp thread, and (d) hemp thread treated for 5 min at 60°C.

More recently, Aiello, et al reported how NFW can be modified to fabricate high surface area, mesoporous (i.e., 2-50 nm pore diameter) biocomposites by using a non-polar solvent gradient following IL removal.[10] Then, Larm, et al revealed how careful selection and/or order of rinse solvents can help tune the surface area and porosity of the final mesoporous biopolymer material.[11] Using this matrix as a scaffold, Larm, et al then showed how silver NPs could be grown within this matrix so they remained encapsulated, yet available for subsequent catalysis.[17] Because the MOFs in this study have diameters within the same range as fiber-welded mesoporous cellulose, they are considered an outstanding candidate for encapsulation within this matrix.[10, 11, 17]

III. Project Goals

The objectives of this project included the following:

(1) Determine the degradation rate of several zirconium-based MOFs containing different encapsulated azole derivatives in the hydrolysis of a nerve-agent simulant.

(2) Incorporate these MOF structures into usable fabrics that protect against organophosphate nerve agent exposure.

Goal 1 was accomplished using ^{31}P nuclear magnetic resonance (NMR) spectroscopy to quantitatively determine the rate of organophosphate nerve agent hydrolysis. Other MOF structural information was elucidated with ^{1}H NMR, nitrogen physisorption analysis, and thermogravimetric analysis (TGA). Goal 2 was accomplished by utilizing a novel method of trapping MOF NP into a natural fiber welded mesoporous cellulose matrix. A UV-Vis spectroscopy method developed in-house was used to monitor the degradation of DMNP by the MOFs trapped in mesoporous cellulose.

IV. Previous Research

a. Synthesis and Catalytic Performance of UiO-67.5

UiO-67.5 MOF derivatives were successfully synthesized and analyzed in 2021 by Professor Whitaker's lab, including UiO-67.5 azobenzene-4,4'-dicarboxylic acid (UiO-67.5 Azo) and UiO-67.5 4,4'-stilbenedicarboxylic acid (UiO-67.5 Stil). Small samples of these MOFs are shown in Figure 6. However, these MOFs required the use of a phosphazene base in aqueous solution to effectively hydrolyze DMNP. Figure 7 shows the ^{31}P NMR spectra for the degradation of DMNP by UiO-67.5 Azo in aqueous solution with and without phosphazene base at a reaction time of 24h.

Figure 6. UiO-67.5 Stil (off-white color) and UiO-67.5 Azo (orange) post synthesis and activation.

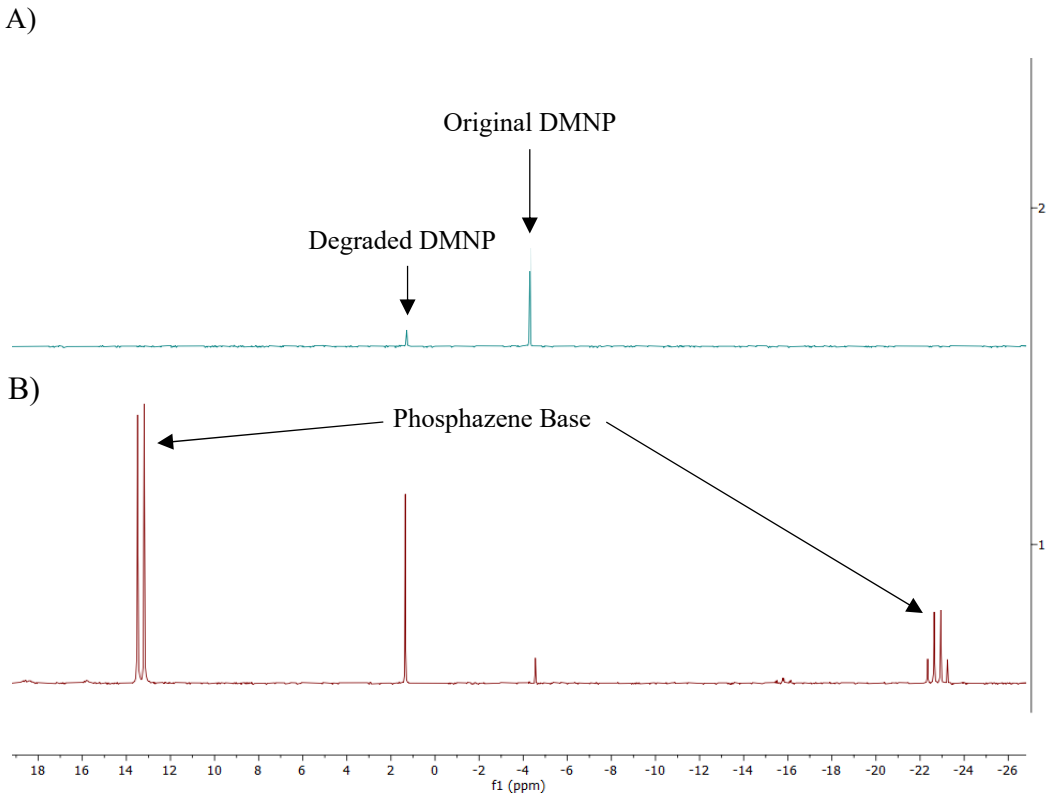

Figure 7. ^{31}P NMR spectra for 24h degradation of DMNP by UiO-67.5 Azo in H_2O (A) without a phosphazene base and (B) with a phosphazene base.

b. Incorporating Azoles into MOF-808

Luo et al showed that imidazole bases incorporated into MOF-808, a zirconium MOF, have enhanced the catalytic degradation of organophosphate nerve agents and reduced the hydrolysis reaction $t_{1/2}$ to <30s ($t_{1/2}$ is the time required for 50% of the nerve agent mimic to be hydrolyzed).[7] The structure of MOF-808 and its degradation mechanism are shown in Figure 8 from Luo et al.[7] New MOF composites were created using a vapor-sorption method, which vaporized imidazole and methyl imidazole into the pores of MOF-808 (Im@MOF-808 denotes imidazole in MOF-808 and MeIm@MOF-808 denotes methyl imidazole in MOF-808). Imidazole and methyl imidazole were heated under vacuum at 120°C and 160°C respectively for 72h in the presence of activated MOF-808 to allow the azoles to enter the pores of MOF-808. FT-IR spectra and BET surface areas were measured and proved the presence of the encapsulated azoles. Quantification of the MOF-azole composites was done using ^{1}H NMR in KOH/D_2O, and yielded 12.2 Im or 9.4 MeIm molecules per MOF-808 unit.[7] The previous synthesis and vapor-sorption techniques were replicated in this project to produce MOF composites of similar yield and purity.

The catalytic activities of Im@MOF-808 and MeIm@MOF-808 toward DMNP hydrolysis in pure H_2O were measured using ^{31}P NMR spectroscopy by tracking the DMNP peak (-4.4 ppm) and the peak of the hydrolyzed product dimethyl phosphate (DMP) (2.8 ppm). Im@MOF-808

showed a 54% conversion within 30 seconds, resembling that of MOF-808 in the presence of a strong base, showing a significant improvement over control experiments. MeIm@MOF-808 had a significantly slower conversion rate (67% conversion after 1 hour), but it is possible this is due to fewer MeIm molecules per MOF-808 unit when compared to Im.[7] This project aimed to extend this research by examining the effects of azole incorporation in UiO-series MOFs (i.e., UiO-67 and UiO-67.5).

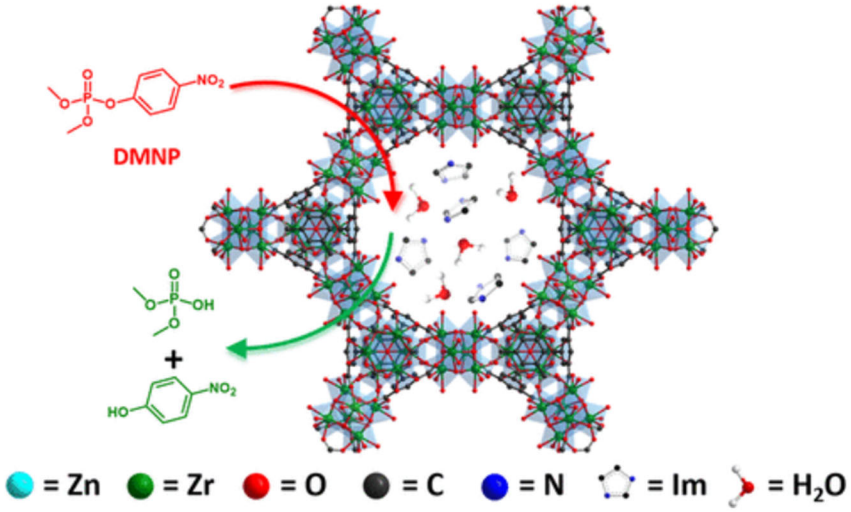

Figure 8. Imidazole incorporated into a pore of MOF-808 along with the simulant breakdown analyzed.

c. Entrapment of TiO_2 Nanoparticles in Fiber-welded Mesoporous Cellulose

In a parallel study that is yet unpublished, TiO_2 NP were encapsulated into a fiber-welded mesoporous cellulose matrix. For this to process to work, the nanomaterial of interest must be (i) suspendable and stable in a solvent that does not collapse the mesoporous matrix prior to NP entrapment and (ii) within the same size range as the mesopores. Because some MOFs in this study fit both criteria, the same methods were employed to trap the MOFs in a similar matrix for our study.

V. Experimental Methods

a. Overview

This experimental study consisted of three phases. Phase I developed new composite MOFs using zirconium-based inorganic nodes, various sizes of organic linkers, and different incorporated azole derivatives. Phase II analyzed the structural properties of the MOFs to determine composition, thermal properties, pore size, and surface area. Additionally, the catalytic performance of MOF powders was evaluated in Phase II. Phase III involved incorporating select MOFs into mesoporous cellulose and evaluating their catalytic performance towards hydrolysis of the DMNP simulant.

b. Chemicals and Equipment

Chemicals used and their manufacturers are as listed: paraoxon methyl (DMNP, Sigma-Aldrich, BCCF7777), hydrofluoric acid (HF, Sigma-Aldrich, MKCK5091, 48%), 4,4'-biphenyldicarboxylic acid (bpydc, Tokyo Chemical Industry, 2L8EJ-AS, >97%), azobenzene-4,4'-dicarboxylic acid (Tokyo Chemical Industry, A8NRI-JG, >95.0%), zirconium(IV) chloride ($ZrCl_4$, Thermo Scientific, W16I009, >99.5%), imidazole (Im, Sigma-Aldrich, WXBD6125V, 99%), 3-amino-1,2,4-triazole (Tokyo Chemical Industry, WMHBA-GB, >98.0%), 1,2,4-triazole (Thermo Scientific, Z13E046, 99%), trimesic acid (Sigma-Aldrich, MKCQ8771, 95%), N,N-dimethylformamide (DMF, Acros Organics, A0369407, 99.8%), methanol (MeOH, Pharmco, C20L14006, HPLC-UV grade), 2',5'-dimethyl-[1,1':4',1"-terphenyl]-4,4"-dicarboxylic acid (Chem Scene, Le0h0485), dimethyl sulfoxide-d6 (dmso-d6, Acros Organics, A0433892, NMR grade), acetic acid (HOAc, Sigma-Aldrich, SHBG5375V, >99%), sodium dodecyl sulfate (SDS, SIGMA, 99%), ethyl-methylimidazolium ethylacetate (EMIAc, Io-Li-Tec, IL-0189-TG, 95%, nominal water content by KF titration is 0.28 wt%), isopropanol (IPA, Aldrich, 190764, ≥99.5%), 2-butanone (2B, Aldrich, 360473, ≥99.0%), cyclohexane (CH, Aldrich, 227048, 99.5%), 4-nitrophenolate (4-NP, Acros Organics, B0150783, 99%), N-ethylmorpholine (NEM, Acros Organics, A0382449, 99%), and 18 MΩ e-pure water (H_2O, Barnstead E-Pure Water Filtration System). All chemicals were certified ACS reagent grade and were used as received unless noted otherwise.

The following textiles were used as received unless noted otherwise: pure cotton cross-stitch fabric aida cloth (22 count, Sensations™).

The following instruments were used through facilities available at the United States Naval Academy: JEOL 400 MHz nuclear magnetic resonance spectrometer, TA Instruments Q500 TGA, Micrometrics ASAP 2020 Plus Physisorption Analyzer, Thermo Fisher Scientific NanoDrop™ UV-Vis Spectrometer. All pH values recorded using calibrated Denver Instrument *Ultra*Basic UB-10 pH Meter and Hydrion® pH paper. N_2 gas was used for surface area measurements and TGA analysis.

c. Phase I: MOF Preparation

The baseline MOFs synthesized included UiO-67, UiO-67.5 Azo, UiO-68, and MOF-808. The organic linkers used in these MOFs are shown in Figure 9. All UiO series and MOF-808 MOFs followed a solvothermal synthesis scheme. 24.0 mg (0.103 mM) $ZrCl_4$, an equimolar amount of dicarboxylic or tricarboxylic acid organic linker, 210 mg acetic acid, and 4 mL DMF were added to a 20 mL glass scintillation vial. Dicarboxylic acid organic linkers were as follows: 4,4'-Biphenyldicarboxylic acid for UiO-67, azobenzene-4,4'-dicarboxylic acid for UiO-67.5 Azo, [1,1':4',1"-terphenyl]-4,4"-dicarboxylic acid for UiO-68, and trimesic acid for MOF-808. The solution was sonicated for 5 minutes, and then the scintillation vial was suspended in a 120°C oil bath for 48h to allow for MOF formation. The initial solution of the MOF-808 starting materials before heating in the oil bath and after 48h at 120°C are shown in Figure 10(A,B).

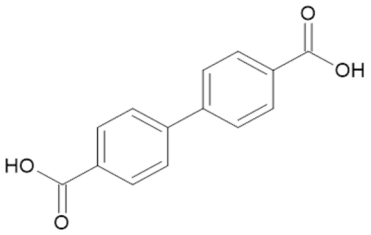

UiO-67 Linker

4,4'-Biphenyldicarboxylic acid

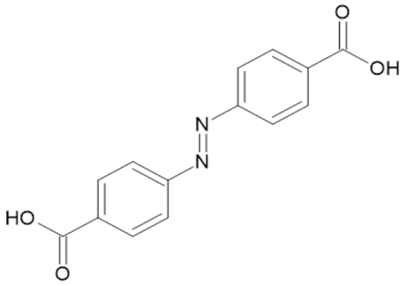

UiO-67.5 Azo Linker

Azobenzene-4,4'-dicarboxylic acid

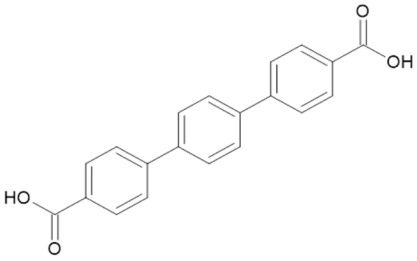

Dimethyl UiO-68 Linker

[1,1':4',1"-Terphenyl]-4,4"-dicarboxylic acid

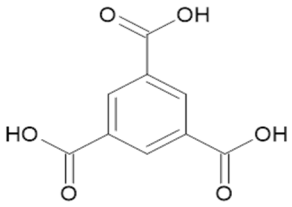

MOF-808 Linker

Trimesic acid

Figure 9. Organic linkers used to synthesize baseline MOFs.

Following heating in the 120°C bath for 48h, the MOF mixture was transferred to a 125 mm threaded test tube using additional DMF. The mixture was centrifuged at 3400 rpm for 10 min. The solvent was decanted and 10 mL of fresh DMF was added once more. The mixture was shaken vigorously and centrifuged for another 10 min. The solvent was decanted, 10 mL of methanol was added, and the tube was shaken vigorously. The MOF soaked in methanol for 48h, as shown in Figure 10(C), then the test tube was centrifuged for 10 minutes and the remaining purified MOF precipitate was isolated. The MOF was placed in a vacuum oven at 120°C under 28 inHg vacuum for 48h to allow for removal of any moisture and excess solvent trapped in the pores. The dry, activated MOF powder, seen in Figure 10(D), was isolated and stored in a vacuum desiccator.

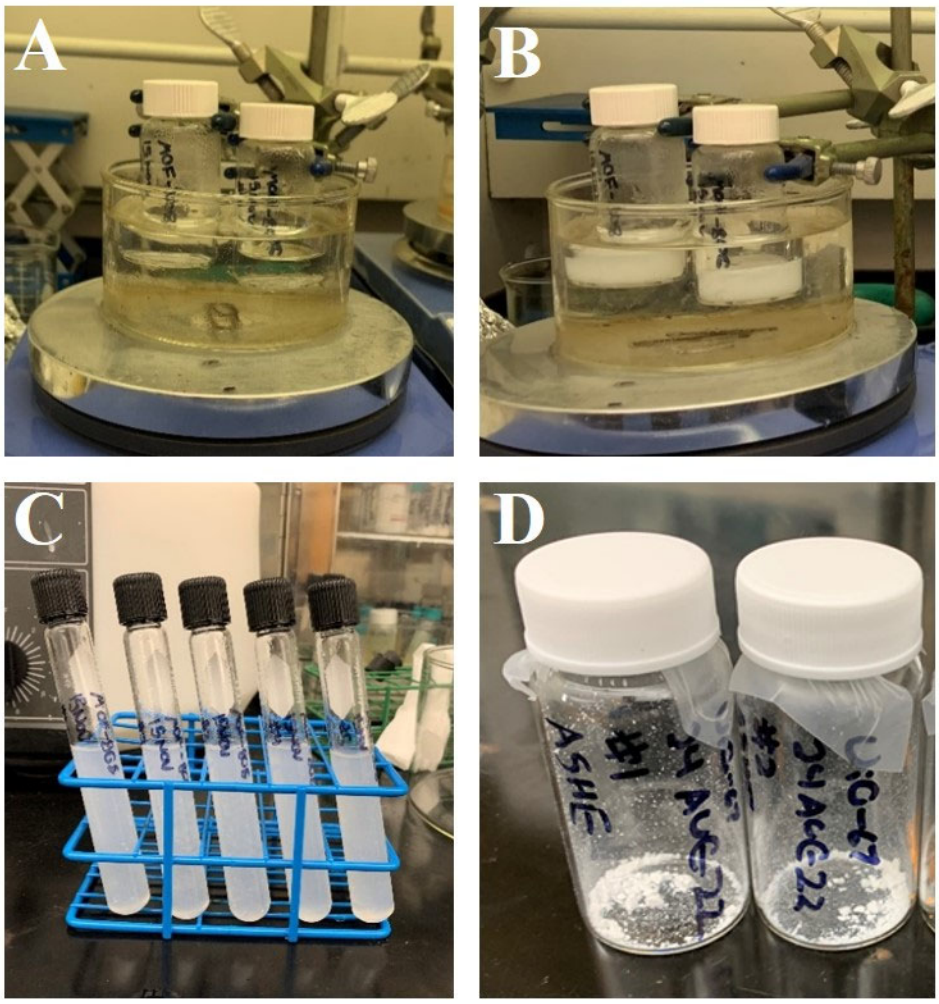

Figure 10. MOF preparation process: A) A solution of $ZrCl_4$, acetic acid, and trimesic acid in DMF upon addition to 120°C oil bath. B) The solution in A showing MOF-808 crystallization after 48h of heat. C) MOF-808 soaked in methanol for 48h. D) UiO-67 MOF following activation (48h at 120°C under vacuum).

d. Phase I: Incorporation of Azoles

The azoles used in this study included imidazole, 1,2,4-triazole, and 3-amino-1,2,4-triazole. Their structures are depicted in Figure 11. Imidazole has the most basic azole structure, consisting of a five-membered ring containing two nitrogen atoms. 1,2,4-triazole adds an additional nitrogen atom to the five-membered ring of the azole. 3-amino-1,2,4-triazole as an extra amino functional group coming off the ring. These three azoles were compared to see how each affects the rate of simulant degradation when incorporated in baseline MOF structures.

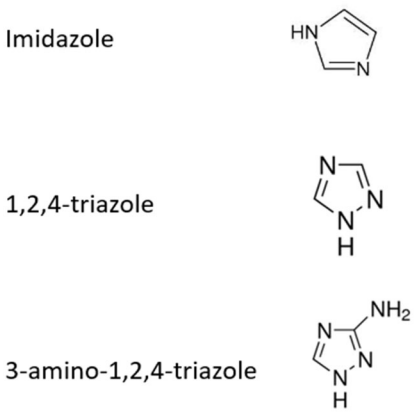

Figure 11. Azoles used in this study.

To incorporate the azole derivatives into the MOF structure, a vapor-sorption method was used. This technique involved using elevated temperature and vacuum to vaporize the azole into the pores of the MOF while maintaining the integrity of the MOF structure. These azoles were then trapped in the framework upon cooling. To do this, an apparatus was constructed as displayed in Figures 12 and 13. In each aluminum foil tray, 15 mg of MOF powder was added and 1.0 g of azole was added to the watch glass. A glass cover was placed over the apparatus in the vacuum oven to prevent escape of the vaporized azole. The apparatus was placed into the vacuum oven at 28 inHg vacuum for 48h at 120°C for imidazole and 140°C for 1,2,4-triazole and 3-amino-1,2,4-triazole. ^{1}H NMR confirmed the addition of azole to the MOF pores without degradation of MOF structure.

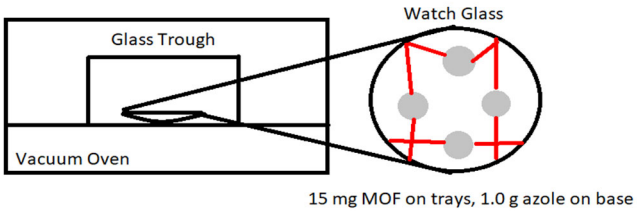

Figure 12. Vapor-Sorption Apparatus Schematic.

Figure 13. Vapor-Sorption Apparatus in Vacuum Oven.

e. Phase I: Qualitative Degradation Tests

5.0 mg of MOF or MOF composite were added to a 20 mL scintillation vial. 4.0 µL of DMNP was added directly to the MOF powder. 1 mL of H_2O was added to the vial and the solution was vigorously shaken followed by sonication for 5 minutes. The mixture reacted for 24h. 50 µL of HF was added to halt the reaction and the solution was sonicated for 5 minutes. It was then

transferred to an NMR tube and ^{31}P NMR was taken of the sample. In the resulting spectrum, a peak with negative shift at approximately -4 ppm was from the unreacted nerve agent simulant DMNP. A peak at approximately +3 ppm appeared upon successful degradation of the simulant. MOFs and MOF composites that did not significantly degrade DMNP in 24h did not continue to Phase II kinetic tests.

f. Phase II: Quantitative Degradation Tests

5.0 mg of MOF or MOF composite was added to nine separate 20 mL scintillation vials. 4 µL of DMNP was added directly to the powder in addition to 1 mL of H_2O. Each vial was designated a specific reaction time: 1, 3, 5, 10, 15, 30, 60, 240, and 1440 minutes. After the designated amount of time had passed, 50 µL HF was added to the corresponding vial to halt the reaction and the solution was analyzed via ^{31}P NMR.

The spectra for each time interval were collected and an overlay of the reaction progress for Im@MOF-808 is shown in Figure 14. This data was then used to construct a percent conversion over time curve that provided the kinetic data such as $t_{1/2}$ for the degradation of the DMNP by the specific MOF/MOF composites.

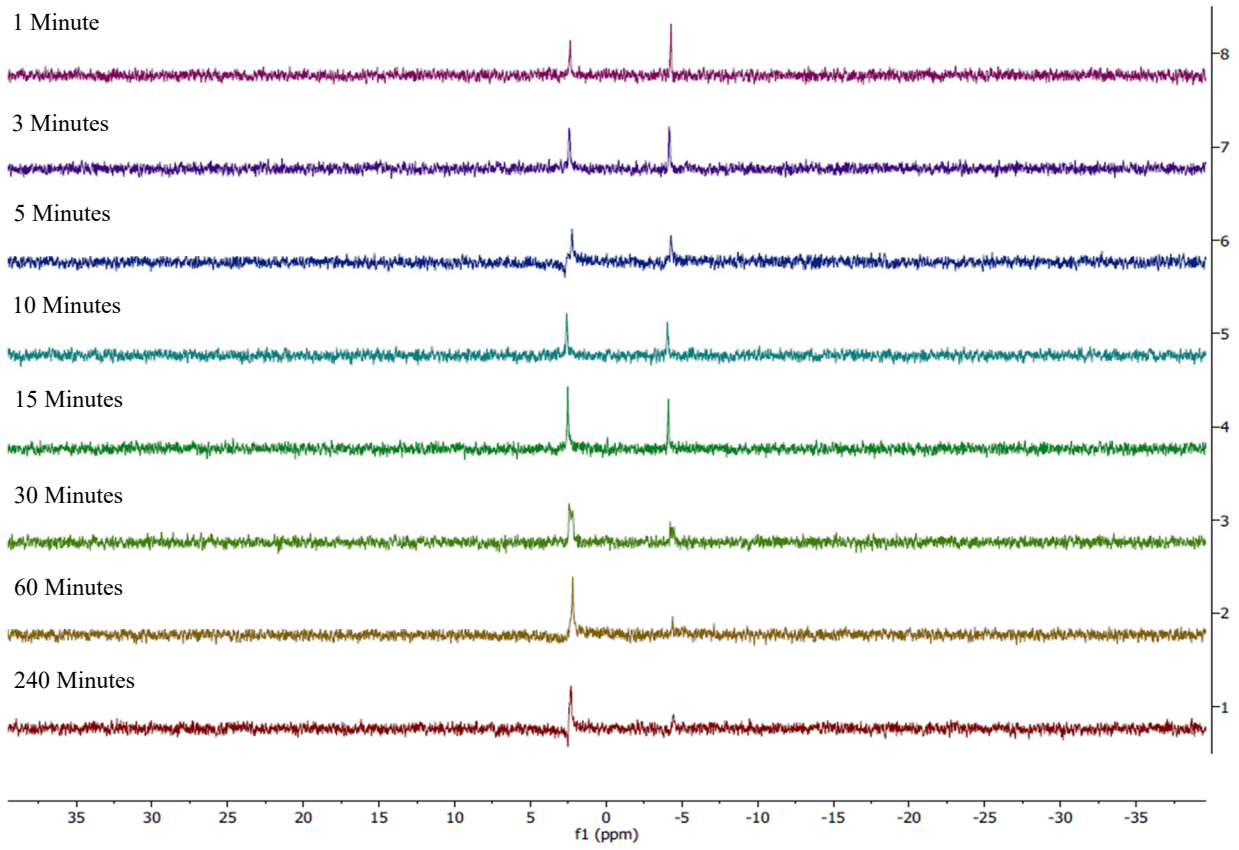

Figure 14. ^{31}P spectra overlay over time for DMNP degradation by Im@MOF-808.

g. Phase III: Trapping MOF into Mesoporous Natural Fiber Welded Cellulose

A schematic of the general loading process of MOFs into NFW mesoporous cellulose is depicted in Figure 15. In step 1, the mesoporous fabric was dipped into a 1 mg mL^{-1} colloidal suspension of MOF for 60s. Mesoporous NFW cellulose was created using the following procedure. Native Aida cloth was submerged in EMIAc (60 min, 60°C), followed by removal from dry box and submergence in H_2O (8 oz, 24h, room temperature), emptying the H_2O and refreshing instantly and after 5, 10, and 60-minute periods as well as following overnight rinse. The samples were then exposed to the solvent gradient of IPA (60 mL, 24h), 2B (60 mL, 24h), and CH (60 mL, 24h), emptying and refreshing solvent after 1 minute. Finally, Aida cloth samples were pressed between Teflon for pre-drying in an oven (60°C, 24h) and samples were transferred to vacuum oven (60°C, 24h) to complete the drying process. All samples were sealed in plastic bags and stored under N_2 before dipping into the colloidal suspension of MOF. In step 2, the fabric was dried at 60°C for 24h followed by 60°C under vacuum for another 24h. Step 3 was a 72h H_2O rinse, exchanging the H_2O every 24h. Step 4 repeated step 2, yielding a mesoporous cellulose-MOF composite. The MOF-laden fabric was stored under H_2O prior to use. This entrapment process was repeated with cellulose that had not undergone NFW (control sample).

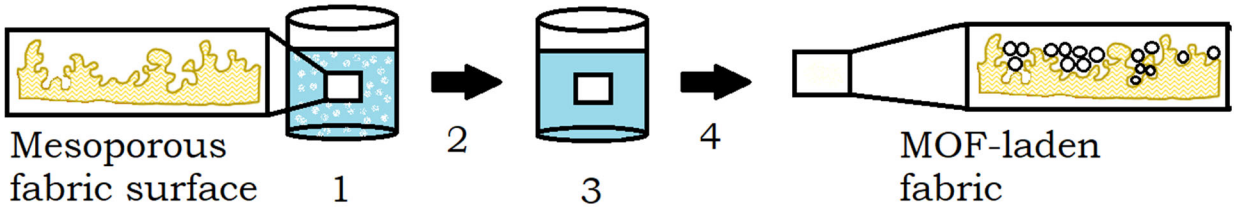

Figure 15. Schematic of MOF loading into NFW mesoporous cellulose.

h. Phase III: Monitor Degradation of DMNP by MOF/Mesoporous Cellulose System

Due to interactions between DMNP degradation products and the cellulose matrix, ^{31}P NMR was ruled out as an acceptable method to evaluate the catalytic efficacy of the MOF-cellulose composites. During DMNP degradation, 4-nitrophenol is formed. The deprotonated form of 4-nitrophenol is 4-nitrophenolate, which absorbs UV-Vis light at 400 nm. The structures of these products are shown in Figure 16. UV-Vis spectroscopy was selected as an alternative method to evaluate the catalytic reaction. When the reaction occurred in a buffered solution that deprotonates the 4-nitrophenol to form 4-nitrophenolate, the reaction progress could be monitored. A sample of the mesoporous cellulose-MOF composite was placed into a 1 mL 0.3 M N-ethylmorpholine (NEM) acetate solution buffered to a pH of 7.00. 10 µL of DMNP was then added into the stirring solution. Every 2 minutes, until the absorbance stopped increasing significantly, a 2 µL aliquot of the reaction solution was placed onto a Nanodrop UV-Vis spectrometer, measuring the absorbance. This process was done for the NFW mesoporous cellulose with MOF, the native cellulose-MOF control, and a control absent fabric or MOF.

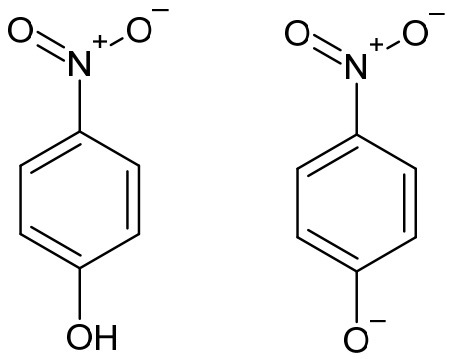

Figure 16. Structures of 4-nitrophenol (left) and 4-nitrophenolate (right).

VI. Data Analysis and Results

a. Confirmation of Azoles in MOFs

^{1}H NMR was used to confirm the vapor-sorption method was successful in incorporating the desired azoles into the MOF structures while maintaining the integrity of the MOF. The ^{1}H NMR spectra were taken for imidazole, 1,2,4-triazole, and 3-amino-1,2,4-triazole. The spectra for UiO-67, UiO-67.5 Azo, UiO-68, and MOF-808 were compared to the MOF composites to analyze whether the azoles were present in the new composites. An example of this with Im@UiO-67.5 Azo is shown in Figure 17. The NMR spectra comparison showed successful incorporation of imidazole into the MOF UiO-67.5 Azo using the described vapor-sorption method. The doublets in the 7.5-8.5 ppm region are from the organic linker molecule. In Im@UiO-67.5 Azo, the imidazole peaks and UiO-67.5 Azo peaks are maintained. The broad peaks at 5.6-6.1 ppm are from the HF used in the NMR solvent. The solvent peaks at 2.46 ppm are from DMSO-*d6*. The peak at 3.35 ppm in Im@UiO-67.5 Azo is from H_2O that has been absorbed by the sample. Detailed data from the spectra in Figure 17 is presented below.

Imidazole. 1H NMR (400 MHz, DMSO-*d6*) δ 8.76 (s, 1H), 7.48 (s, 2H), 6.10 (bs), 2.46 (s).

UiO-67.5 Azo. 1H NMR (400 MHz, DMSO-*d6*) δ 8.11 (d, J = 8.00 Hz, 4H), 7.95 (d, J = 8.00Hz, 4H), 5.66 (bs), 2.46 (s).

Im@UiO-67.5 Azo. 1H NMR (400 MHz, DMSO-*d6*) δ 8.93 (s, 1H), 8.11 (d, J=8.00 Hz, 4H), 7.95 (d, J = 8.00Hz, 4H), 7.57 (s, 2H), 5.73 (bs), 3.35 (s), 2.46 (s).

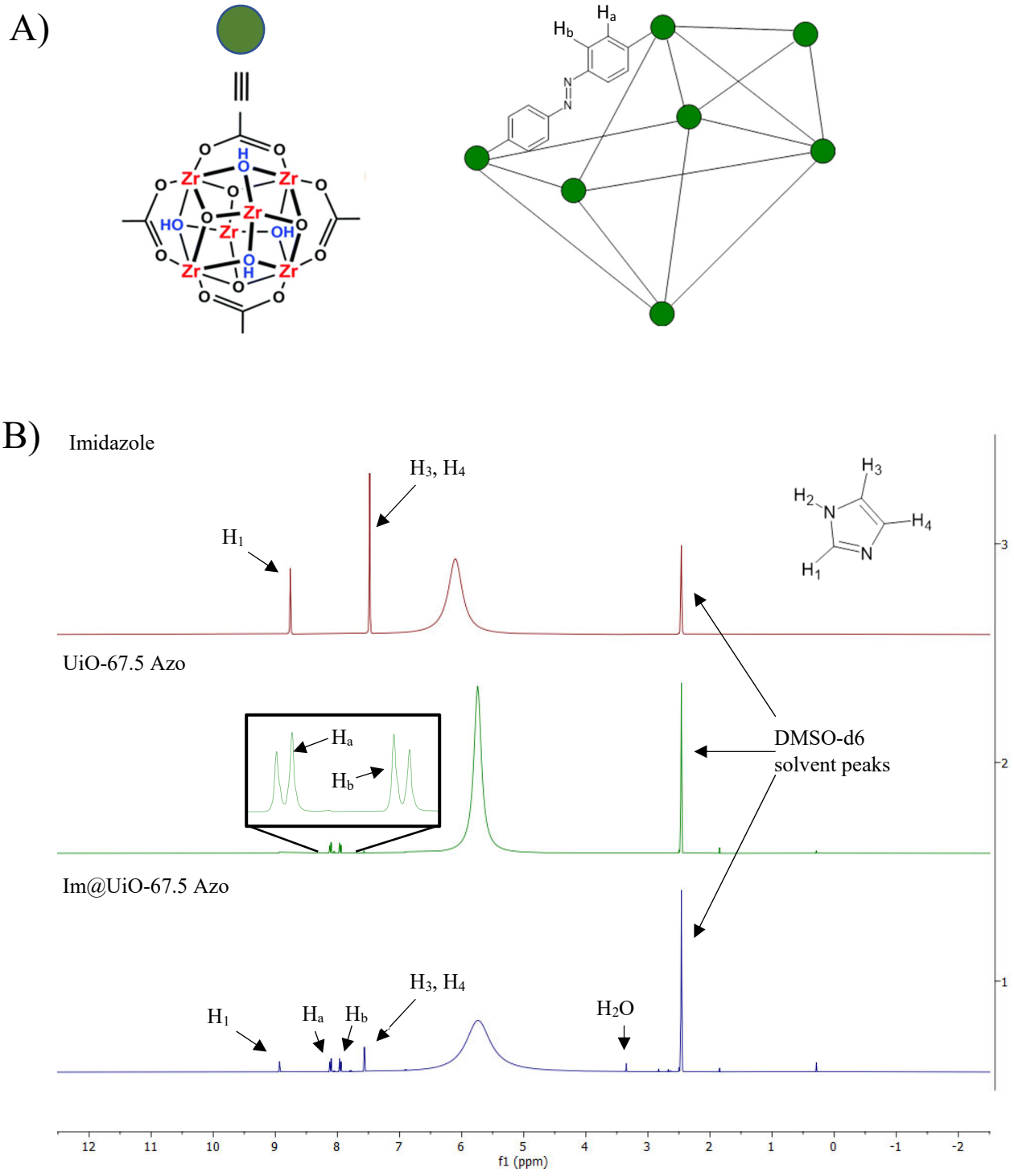

Figure 17. Structure of UiO-67.5 Azo (A) and ^{1}H NMR spectra stack of imidazole, UiO-67.5 Azo, and Im@UiO-67.5 Azo (B).

b. Qualitative Degradation Tests

Qualitative tests showed varying success in degradation of DMNP by MOF composites over a period of 24h. Similar spectra to those seen in Figures 7 and 15 were used to give % degradation in this time interval. Table I shows a summary of DMNP degradation percentages for the family of MOF composites. All UiO-68 MOF composites showed minimal degradation of ≤40% conversion at 24h. Additionally, all baseline MOFs containing 1,2,4-triazole showed ≤35% conversion. Therefore, all UiO-68 and 1,2,4-triazole incorporated MOF composites were not pursued further. Im@MOF-808, Im@UiO-67.5 Azo, 3-Amino-1,2,4-triazole@MOF-808, and 3-Amino-1,2,4-triazole@UiO-67.5 Azo MOF composites showed promising 100% conversions over a period of 24h. Im@UiO-67 and 3-Amino-1,2,4-triazole@UiO-67 degraded over half of the DMNP in 24h. Based on these results, UiO-67, UiO-67.5 Azo, and MOF-808 containing imidazole and 3-amino-1,2,4-triazole were chosen for quantitative testing.

Table I. Qualitative Evaluation of MOF Ability to Degrade DMNP

Baseline MOF	Azole Derivative	DMNP Degradation % (24h)	Quantitative Testing?
UiO-67	Imidazole	55	Yes
	1,2,4-Triazole	20	No
	3-Amino-1,2,4-Triazole	60	Yes
UiO-67.5 Azo	Imidazole	100	Yes
	1,2,4-Triazole	0	No
	3-Amino-1,2,4-Triazole	100	Yes
UiO-68	Imidazole	40	No
	1,2,4-Triazole	0	No
	3-Amino-1,2,4-Triazole	20	No
MOF-808	Imidazole	100	Yes
	1,2,4-Triazole	35	No
	3-Amino-1,2,4-Triazole	100	Yes

c. Thermal Analysis of MOFs Using Thermogravimetric Analysis (TGA)

TGA data was used to determine MOF thermal stability and solvent retention. The TGA data are shown in Figure 18 and summarized in Table II. Data were collected under N_2 at 10°C min^{-1}. T_5 is the temperature at which 5% of mass has been lost during the temperature ramp. Wt% solvent is mass evolved by 135°C. $T_{d,\,max}$ is the maximum decomposition temperature. UiO-67 and UiO-67.5 Azo have little degradation under 500°C. MOF-808 shows a more gradual decomposition from 250°C to 550°C. This was expected and closely resembles previous literature reported values.[7]

Table II. Baseline MOF TGA Data

MOF	T_5 (°C)	Wt% Solvent	$T_{d,\ max}$ (°C)
UiO-67	255	3.01	569
UiO-67.5 Azo	224	1.63	551
MOF-808	271	3.80	557

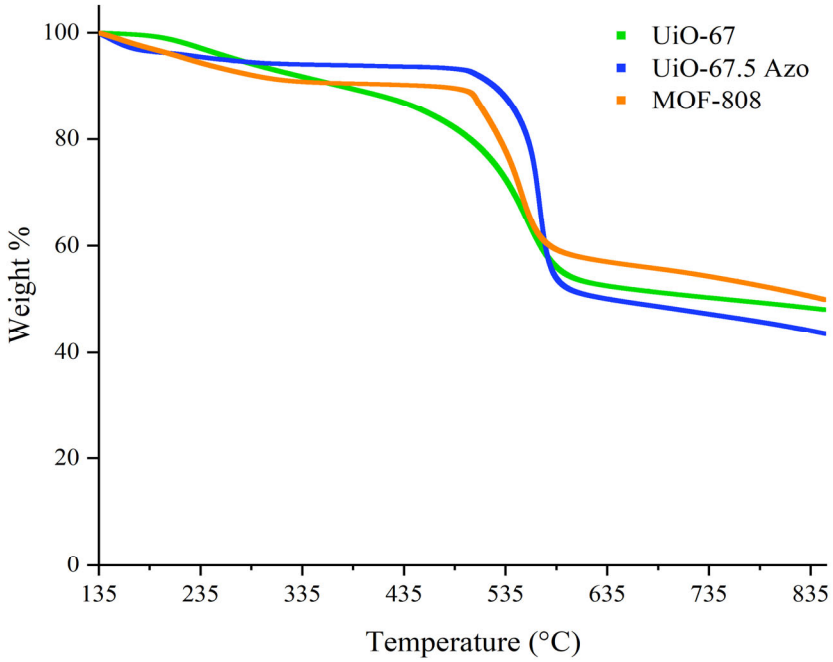

Figure 18. TGA curves for baseline MOFs from 135°C to 850°C at a temperature ramp of 10°C min^{-1}.

Initial TGA of the MOFs showed that there were significant amounts of H_2O and solvent remaining in the MOF porous framework when 60°C was used as the activation temperature (final drying temperature to evacuate pores of the MOF). The excess solvent would block the pores and prevent interaction of the MOF nodes with the nerve agent simulant. The activation temperature was increased to 120°C to remove the excess solvent without degrading the MOF structure. Drying at 60°C under vacuum for 48h resulted in >40% of the UiO-67's mass being H_2O and residual solvent. Drying at 120°C under vacuum for 48h decreased this to 3.01% by mass.

d. Physisorption Measurements of MOFs

The N_2 adsorption-desorption isotherms for UiO-67, UiO-67.5 Azo, and MOF-808 are shown in Figure 19. Table III summarizes the Brunauer-Emmett-Teller (BET) surface area and pore sizes of these MOFs. All MOFs show Type IV isotherms, indicating they are mesoporous. A larger average pore size was observed in MOF-808 (compared to UiO-67 and UiO-67.5 Azo).

These data make sense, as MOF-808 linkers are tricarboxylic acid, whereas the UiO series linked by dicarboxylic acids. Interestingly, MOF-808 also has the lowest BET surface area perhaps due to more crosslinking.

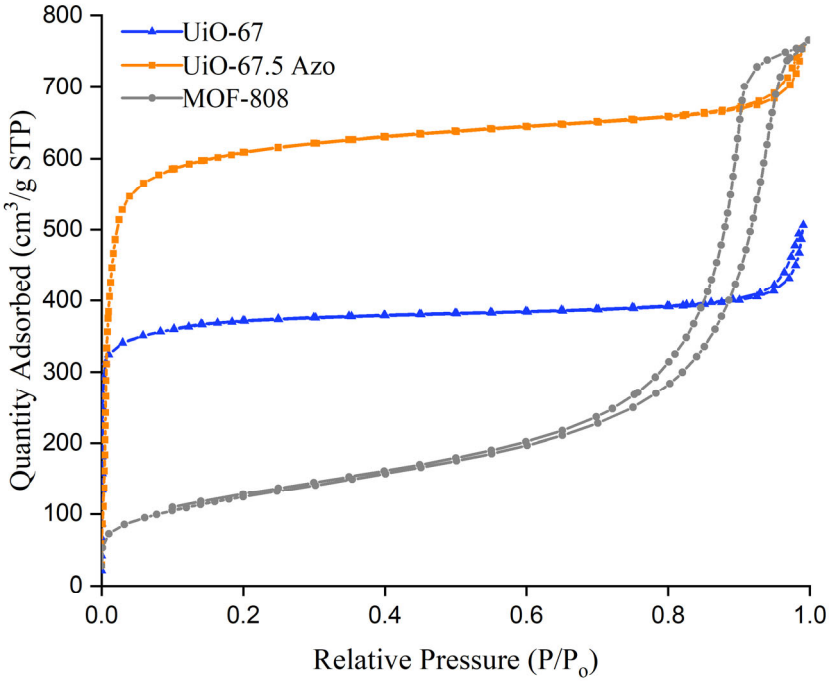

Figure 19. N_2 Adsorption-Desorption Isotherms of UiO-67, UiO-67.5 Azo, and MOF-808 used for BET surface area calculation.

Table III. MOF Physisorption Data

MOF	BET Surface Area ($m^2 g^{-1}$)	Pore Diameter (nm)
UiO-67	1,330.4	2.3
UiO-67.5 Azo	2,176.1	2.1
MOF-808	450.6	10.4

e. Quantitative Degradation Tests

The percentage of DMNP hydrolyzed as a function of time for several MOFs and MOF-composites is shown in Figures 20-22. The relevant kinetic data are summarized in Table IV. While baseline MOF-808 had much faster degradation kinetics than baseline UiO-67.5 Azo, incorporation of imidazole into both structures resulted in similar kinetic gains. Thus, addition of imidazole to UiO-67.5 Azo had a greater improvement in reaction kinetics when compared to MOF-808. Incorporation of 3-amino-1,2,4-triazole in the MOF composites only improved the reaction rate in UiO-67.5, but did not improve the reaction rate in MOF-808. Both azoles in UiO-67 showed no improvement in reaction kinetics for the degradation of DMNP.

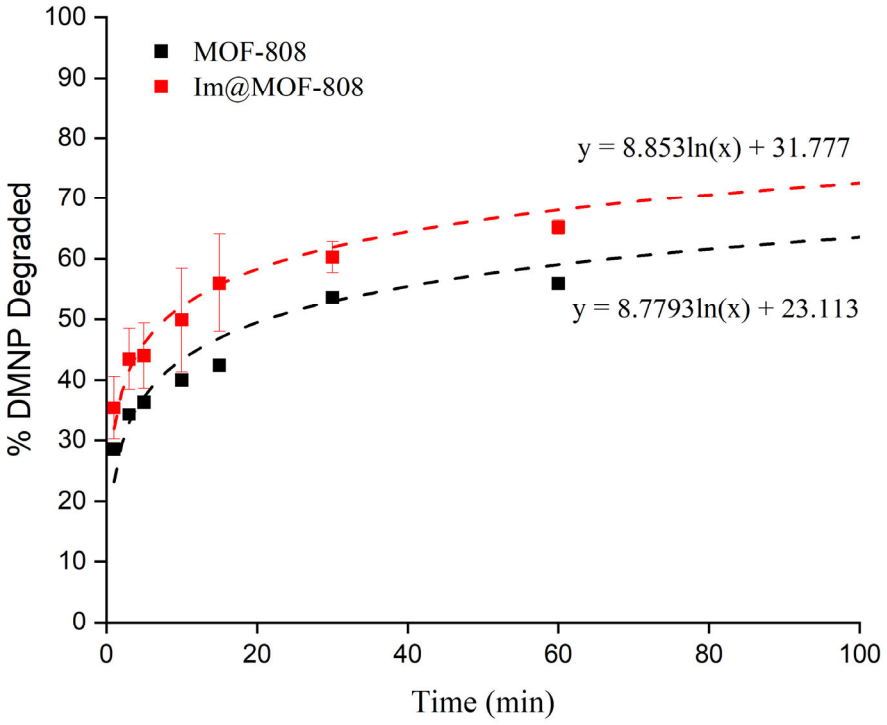

Figure 20. DMNP degradation over time by Im@MOF-808 compared to MOF-808.

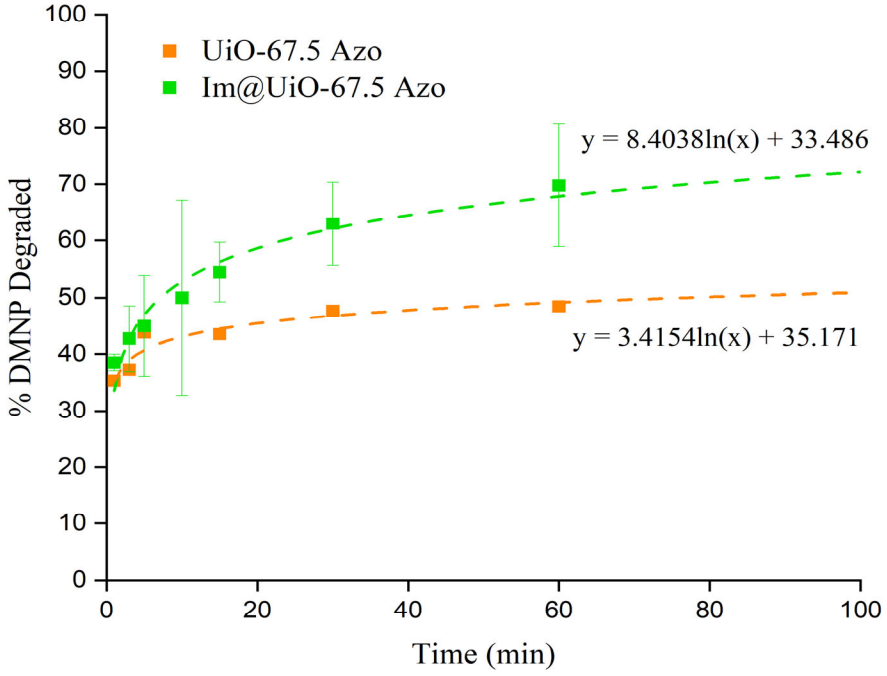

Figure 21. DMNP degradation over time by Im@UiO-67.5 Azo compared to UiO-67.5.

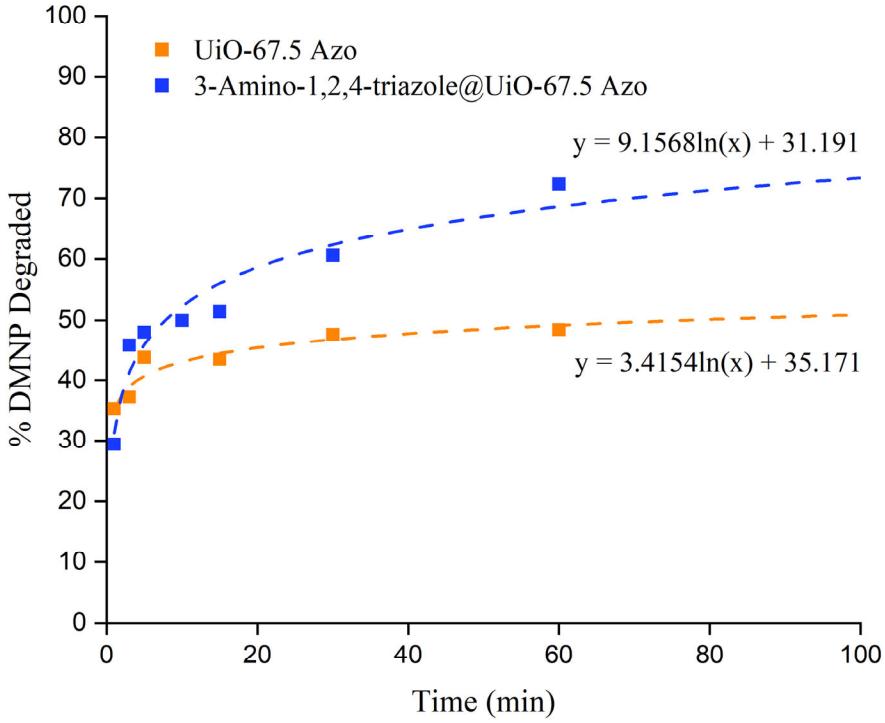

Figure 22. DMNP Degradation over time of 3-Amino-1,2,4-triazole@UiO-67.5 Azo compared to UiO-67.5 Azo.

Table IV. Reaction half-lives for MOFs and MOF composites

MOF/MOF-Composite	$t_{1/2}$ (min)
UiO-67	19
UiO-67.5 Azo	77
MOF-808	21
Im@UiO-67	63
Im@UiO-67.5 Azo	7
3-Amino-1,2,4-triazole@UiO-67.5 Azo	8
Im@MOF-808	8
3-Amino-1,2,4-triazole@MOF-808	28

f. MOF Performance in Mesoporous Cellulose

Initially, UiO-67 and MOF-808 were evaluated for their ability to suspend in water, so they could be encapsulated in the mesoporous cellulose matrix. While UiO-67 suspended easily at a concentration of 1 mg mL^{-1}, MOF-808 did not. Therefore, UiO-67 was chosen for incorporation

into the NFW materials. Scanning electron microscopy (SEM) images of the MOF-mesoporous cellulose system can be seen in Figure 23. Figure 23(i) shows a high-resolution image of the MOFs as they appear on the surface of the mesoporous cotton fabric. Note, these MOFs are what remained after the vigorous (3-day) rinsing procedure used to remove any that were not truly encapsulated. These SEM images show some MOF aggregation at the surface. Figure 23(ii) highlights how the MOFs (i.e., the light-colored dots throughout the image) became integrated within the cross-section of the welded fibers after the encapsulation process was complete. Figure 23(iv) shows an energy dispersive X-ray spectroscopy (EDS) map and spectra of zirconium atoms (in the inorganic nodes of the MOF) from the region of Figure 23(iii), once again proving the MOF is embedded in the matrix.

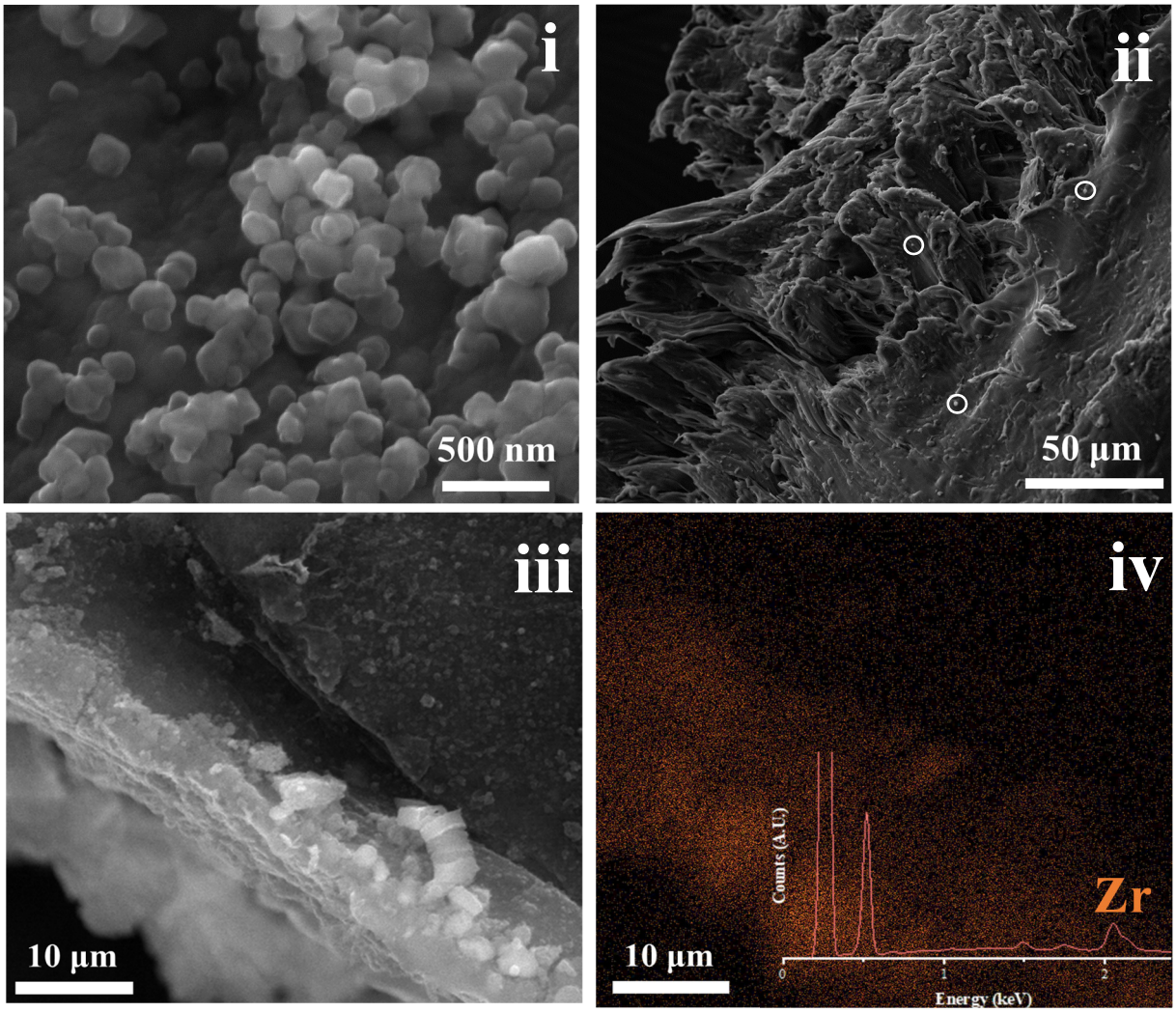

Figure 23. Scanning electron microscopy (SEM) showing (i) high resolution image of MOF UiO-67 that was integrated within the mesoporous NFW fabric, (ii) lower resolution image of UiO-67 integrated within the welded fiber cross section, (iii) image of cross-sectional area mapped using energy dispersive X-ray spectroscopy (EDS) and (iv) the EDS map and spectra of region featured in (iii), highlighting the zirconium metal (from UiO-67) distributed throughout the matrix. The mesoporous biopolymer textile was treated with 1 mg mL^{-1} UiO-67 suspension.

UV-Vis spectroscopy was used to analyze how well the MOFs hydrolyzed the nerve agent mimic DMNP. The spectra for the degradation of DMNP in two-minute time intervals by UiO-67 in NFW mesoporous cellulose is shown in Figure 24. UiO-67 in native cellulose and the control (buffer alone) also degraded DMNP to completion. However, the rate at which this reaction progressed was significantly higher for UiO-67 in NFW mesoporous cellulose when compared to the other two. The standardized catalytic enhancement (%/g) was calculated as follows. At each time interval, the percent reaction completion was calculated. The percent reaction completion for the control was subtracted from the aforementioned value. After this, a mass correction was applied to the remaining percent reaction completion (due to the higher mass of NFW mesoporous cellulose used). These mass corrected enhancements were summed during the extent of the reaction and are shown in Figure 25.

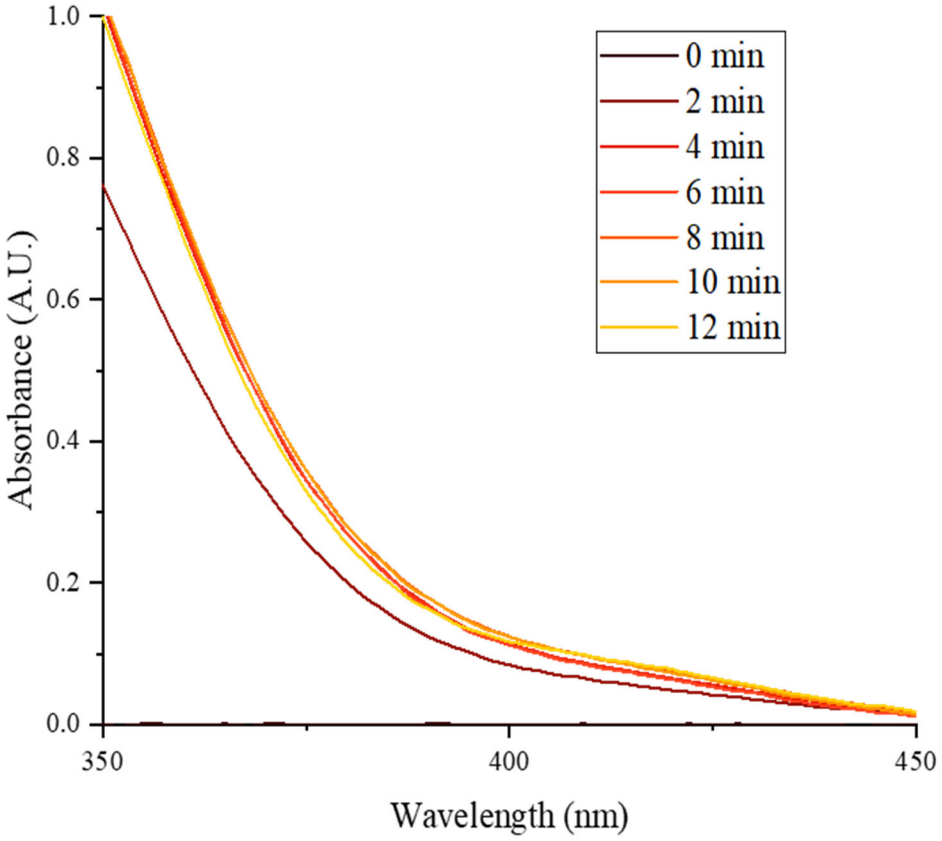

Figure 24. Spectra overlay of 4-nitrophenolate formation catalyzed by UiO-67 in NFW mesoporous cellulose fiber.

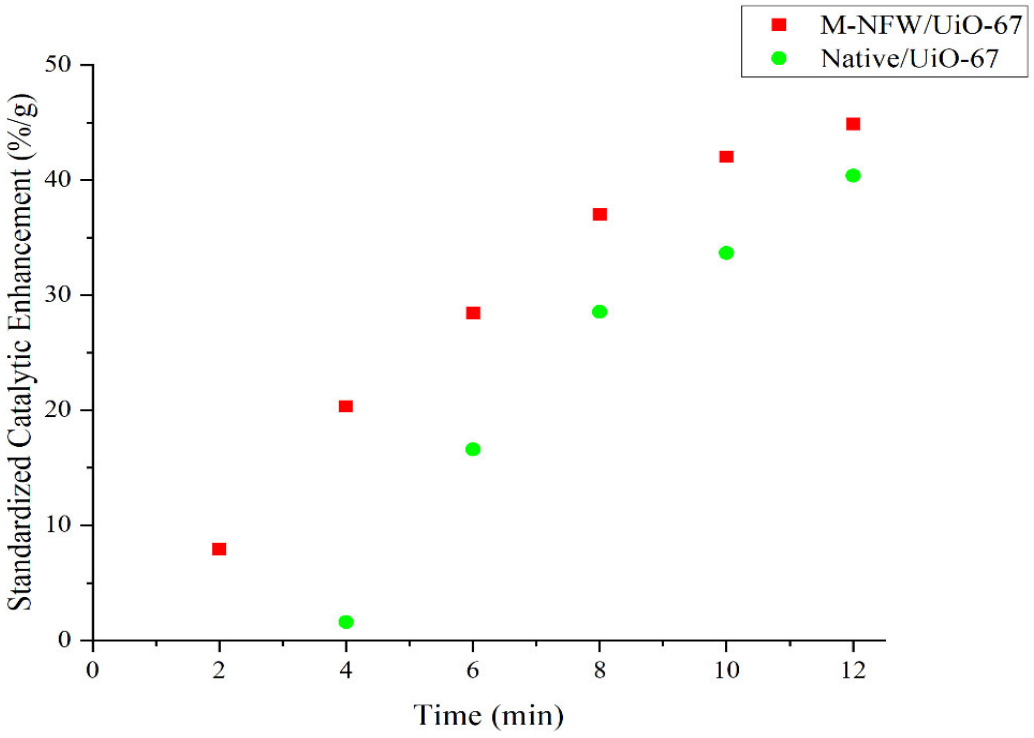

Figure 25. Comparison of UiO-67 in NFW mesoporous cellulose catalytic enhancement of degradation of DMNP compared to UiO-67 in native cellulose.

VII. Discussion

a. Effectiveness of MOF Composites

The method used to incorporate azoles in baseline MOFs was simple and highly effective. Qualitative testing showed that UiO-67, UiO-67.5 Azo, and MOF-808 composites were most successful in degrading the nerve agent simulant DMNP. UiO-68 did not yield enough conversion to warrant further investigation. UiO-68 has the largest organic linker, creating a larger pore size which may have been too big to effectively trap the DMNP molecules and allow them to efficiently interact with the inorganic nodes. The other MOFs have smaller cavities in-between inorganic nodes, which allows more DMNP to encounter the inorganic nodes. Of the three azoles incorporated into the baseline MOFs, imidazole and 3-amino-1,2,4-triazole in UiO-67, UiO-67.5 Azo, and MOF-808 were most successful in degradation of the nerve agent simulant, yielding as high as 100% conversion over a 24h period. 1,2,4-Triazole did not yield results warranting further investigation and hindered hydrolysis of DMNP compared to the baseline MOF. It is worth noting that the 1,2,4-triazole had much larger crystals than imidazole and 3-amino-1,2,4-triazole.

b. Characterization of MOF Composites

During TGA and NMR analysis of the MOF composites, it was discovered that more residual solvent was in the MOF than originally predicted. When dried at 60°C in a vacuum, up to 40% of the MOF weight was solvent and H_2O. The MOFs are extremely hygroscopic and pick up H_2O quickly from the environment (which could be of interest for future studies). A temperature of 120°C was ultimately used for drying the MOFs, which better removed solvents and H_2O. TGA and NMR results for before and after azole incorporation indicated that MOF structural integrity was maintained through the incorporation of azoles. The BET data showed the MOFs synthesized were mesoporous (i.e., pores 2-50 nm diameter) and had high surface areas. Of note, the surface areas obtained for UiO-67 and MOF-808 were lower than previously reported literature reports.[7, 18] Possible explanations for the discrepancies are differences in synthetic procedures coupled with MOF imperfections. For effective catalysis of DMNP degradation, there must be defects in the MOF structure. Lower inorganic node connectivity increases the number of catalytic active sites and leads to better kinetics.[19] MOF degradation may also be occurring upon exposure to ambient lab conditions, which occurred prior to degassing for BET.

c. Kinetics of Simulant Degradation

Incorporating imidazole into MOF-808 improved the MOFs catalytic DMNP degradation, reducing $t_{1/2}$ by >250% (from 21 min to 8 min). Incorporation of imidazole into UiO-67.5 resulted in a similar $t_{1/2}$ of 7 min. This was a much larger improvement from $t_{1/2}$ of 77 min for the parent UiO-67.5. 3-Amino-1,2,4-triazole did improve performance in UiO-67.5 Azo, but to a lesser degree than imidazole. Incorporating more azole moieties in the pores of the MOFs could better facilitate the degradation reaction.[7] An ideal MOF composite would be able to degrade the nerve agent mimic immediately upon exposure. While these results were not obtained, the time required for degradation was significantly reduced compared to the baseline MOFs and approaches the fastest degradation rates for DMNP in the literature.[7]

d. MOF Performance in Mesoporous NFW Cellulose

MOF integration in the mesoporous NFW cellulose was confirmed through both SEM and EDS. The MOF-cellulose system was stored under H_2O for >1 month before the tests were completed. The NFW cellulose system was shown to effectively retain the MOF NP. 1 mg mL^{-1} UiO-67 in H_2O was the only concentration used for the dipping solution due to limited MOF available. Higher loading may be possible if higher concentrations of UiO-67 are able to suspend in solution, though this was beyond the scope of the current study. Suspension in H_2O is not possible for all MOFs (i.e., MOF-808 did not suspend well in H_2O and was not evaluated in mesoporous cellulose) and different solvents should be used to aid solution formation. Altering the solvent polarity may permit better suspension of the MOFs in solution. Full DMNP degradation did not occur in the method, which was probably due to limited MOF composite loading. MOFs incorporated in NFW mesoporous cellulose had better catalytic efficiency than the MOFs in native cellulose when tested in a NEM acetate buffer solution. The increased surface area from the NFW process allowed for this to occur more rapidly. Through capillary action, the mesoporous NFW cellulose clearly entrapped UiO-67 onto the surface and within the cross-section of welded fibers of the fabric while still allowing the MOF composite to catalyze the hydrolysis of DMNP. This is

the first example of a MOF composite being incorporated into a NFW fabric which is able to effectively hydrolyze an organophosphate nerve agent simulant.

VIII. Future Work

All kinetic tests were performed under aqueous conditions. Further studies should be performed to test the MOF composites viability to degrade nerve agents under ambient environmental conditions (dry and controlled relative humidity). Preferably, a facility that has the ability to run solid-state NMR should undertake these efforts. H_2O in some form, whether liquid or vapor, is necessary for the hydrolysis reaction to take place. Theoretically, there is a threshold humidity under which the reaction will not occur at relevant rates. Since many military operations take place in desert environments, work should continue to make MOF composites capable of degrading organophosphate nerve agents in these arid conditions. Additionally, no actual nerve agents were used in testing. All kinetics were analyzed using the nerve agent simulant DMNP. Actual catalytic studies using various types of nerve agents should be performed by trained professionals in proper lab facilities.

Incorporating MOFs into NFW mesoporous cellulose scaffolding showed great potential for real world applications. Filter tests containing this fabric should be performed to determine its viability in applications such as gas mask filters and CBRN filters onboard military craft. Additionally, the method of monitoring DMNP degradation should be evaluated. Ideally, a method that can monitor the reaction without the need for an NEM acetate buffer would be ideal, since this buffer contributed to some degradation of the DMNP.

IX. Conclusions

Azoles were successfully incorporated non-covalently into the pores of zirconium-based MOFs in the UiO series and MOF-808 using a developed vapor-sorption method. Of the MOF composites created, Im@UiO-67.5 Azo, Im@MOF-808, and 3-Amino-1,2,4-triazole@UiO-67.5 Azo provided the greatest kinetic enhancement for nerve agent simulant degradation when compared to the baseline MOFs. UiO-68 composites and composites containing 1,2,4-triazole did not yield efficient enough degradation of DMNP to warrant further study. Incorporation of azoles into the pores of MOFs does not alter the structure of the MOF itself, but alters the microenvironment present at the inorganic nodes. This is what allows the degradation of DMNP to occur at higher rates in the presence of azoles.

The first major goal of this project was to determine the catalytic efficiency of several zirconium-based MOF frameworks with azole derivatives incorporated. The quantitative method developed allowed for successful determination of relevant kinetics. Using this method, it was discovered that the incorporation of imidazole into MOF-808 resulted in a >250% increase in the reaction rate to degrade DMNP simulant compared to MOF-808. Imidazole in UiO-67.5 Azo had over an order of magnitude faster DMNP degradation reaction rate than UiO-67.5, and 3-amino-1,2,4-triazole in UiO-67.5 Azo had a >950% increase in reaction rate. These rates approach some of the fastest found in literature, while having the added benefit that the MOFs used do not require

challenging conditions to synthesize.[7] These results support a central hypothesis of this study: incorporating non-volatile azoles into the pores of Zr-based MOFs yields better reaction kinetics.

A novel method was created to embed UiO-67 into NFW mesoporous cellulose scaffolding. These MOF nanoparticles were able to enhance the rate of DMNP degradation in the mesoporous cellulose fabric to a higher degree than the MOF in native cellulose. NFW materials can be implemented into clothing and other applications. This method could provide a new form of filtration both for gas masks and in military craft engaged in operations involving chemical warfare.

X. Relevance to Navy, DOD, and US

As detailed by the 2018 National Defense Strategy, the central challenge to U.S. prosperity and security is the reemergence of long-term, strategic competition by revisionist powers such as China and Russia.[20] Coupled with this is the danger posed by non-state actors seizing power in regions where a power vacuum is present, such as the Taliban taking Afghanistan in 2021 from the Afghan government following U.S. withdrawal from the region.[21] During this period of inflection in military strategy and tactics, one thing remains constant. The danger of asymmetric warfare tactics is and will remain a threat to both military assets and civilian populations. Although outlawed in warfare by the 1925 Geneva Protocol, nerve agents are still used to commit atrocious acts of violence against individuals and populations.[22] By developing methods and products capable of rendering a poisoned environment safe or delaying the onset of serious symptoms, the U.S. can remain a powerful fighting force in the face of these attacks. Chemical warfare will always exist if individuals with misguided ingenuity devise new methods of attack. It is therefore necessary to continue research and development into antidotes and protection against these methods.

References

(1) Gupta, R. C. Classification and Uses of Organophosphates and Carbamates. In *Toxicology of Organophosphate and Carbamate Compounds*, Elsevier, 2006; pp 5-24.

(2) Figueiredo, T. H.; Apland, J. P.; Braga, M. F. M.; Marini, A. M. Acute and long-term consequences of exposure to organophosphate nerve agents in humans. *Epilepsia* **2018**, *59*, 92-99.

(3) Venturi, D. M.; Campana, F.; Marmottini, F.; Costantino, F.; Vaccaro, L. Extensive Screening of Green Solvents for Safe and Sustainable UiO-66 Synthesis. *ACS Sustainable Chem. Eng.* **2020**, *8* (46), 17154-17164.

(4) Sakamaki, Y.; Tsuji, M.; Heidrick, Z.; Watson, O.; Durchman, J.; Salmon, C.; Burgin, S. R.; Beyzavi, H. Preparation and applications of metal-organic frameworks (MOFs): a laboratory activity and demonstration for high school and/or undergraduate students. *Journal of Chemical Education* **2020**, *97* (4), 1109-1116.

(5) Gil-San-Millan, R.; López-Maya, E.; Platero-Prats, A. E.; Torres-Pérez, V.; Delgado, P.; Augustyniak, A. W.; Kim, M. K.; Lee, H. W.; Ryu, S. G.; Navarro, J. A. R. Magnesium exchanged zirconium metal-organic frameworks with improved detoxification properties of nerve agents. *Journal of the American Chemical Society* **2019**, *141* (30), 11801-11805.

(6) Ma, K.; Wasson, M. C.; Wang, X.; Zhang, X.; Idrees, K. B.; Chen, Z.; Wu, Y.; Lee, S.; Cao, R.; Chen, Y.; et al. Near-instantaneous catalytic hydrolysis of organophosphorus nerve agents with zirconium-based MOF/hydrogel composites. *Chem. Catalysis* **2021**, *1* (3), 502-504.

(7) Luo, H.; Castro, A. J.; Wasson, M. C.; Flores, W.; Farha, O. K.; Liu, Y. Rapid, biomimetic degradation of a nerve agent simulant by incorporating imidazole bases into a metal-organic framework. *ACS Catalysis* **2021**, *11* (3), 1424-1429.

(8) Morgan, S. E.; O'Connell, A. M.; Jansson, A.; Peterson, G. W.; Mahle, J. J.; Eldred, T. B.; Gao, W.; Parsons, G. N. Stretchable and multi-metal-organic framework fabrics via high-yield rapid sorption-vapor synthesis and their application in chemical warfare agent hydrolysis. *ACS Applied Materials & Interfaces* **2021**, *13* (26), 31279-31284.

(9) Guo, Z.; Ren, P.; Yang, F.; Wu, T.; Zhang, L.; Chen, Z.; Huang, S.; Ren, F. MOF-derived Co/C and MXene co-decorated cellulose-derived hybrid carbon aerogel with a multi-interface architecture toward absorption-dominated ultra-efficient electromagnetic interference shielding. *ACS Applied Materials & Interfaces* **2023**, *15* (5), 7308-7318.

(10) Aiello, A.; Cosby, T.; McFarland, J.; Durkin, D. P.; Trulove, P. C. Mesoporous xerogel cellulose composites from biorenewable natural cotton fibers. *Carbohydr. Polym.* **2022**, *282*. DOI: https://doi.org/10.1016/j.carbpol.2021.119040.

(11) Larm, N. E.; Chase, M. A.; Stachurski, C. D.; Gulbrandson, A. J.; Durkin, D. P.; Trulove, P. C. Tunable porosity of cotton xerogels via ionic liquid-based natural fiber welding. *Journal of Material Science* **2022**, *57*, 21841-21852.

(12) Costanzi, S.; Machado, J.; Mitchell, M. Nerve Agents: What They Are, How They Work, How to Counter Them. *ACS Chemical Neuroscience* **2018**, *9* (5), 873-885.

(13) Lawrence, M. C.; Schneider, C.; Katz, M. J. Determining the structural stability of UiO-67 with respect to time: a solid-state NMR investigation. *Chem. Commun.* **2016**, *52*, 4971-4974.

(14) Haverhals, L. M.; De Long, H. C.; Reichert, W. M.; Trulove, P. C. Natural Fiber Welding, U.S. Patent 8,202,379. 2012.

(15) Haverhals, L. M.; Isaacs, T. A.; Page, E. C.; Reichert, W. M.; De Long, H. C.; Trulove, P. C. Ionic liquids in the preparation of biopolymer composite materials. *Electrochemical Society Transactions* **2009**, *16* (49), 129-139.

(16) Haverhals, L. M.; Reichert, W. M.; De Long, H. C.; Trulove, P. C. Natural fiber welding. *Macromolecular Materials and Engineering* **2010**, *295* (5), 425-430.

(17) Larm, N. E.; Gulbrandson, A. J.; Stachurski, C. D.; Chase, M. A.; Trulove, P. C.; Durkin, D. P. Mesoporous natural fiber welded cellulose containing silver nanoparticles as a recyclable heterogeneous catalyst. *Macromol. Mater. Eng.* **2023**, *308* (4), 2370007. DOI: https://doi.org/10.1002/mame.202370007.

(18) Katz, M. J.; Brown, Z. J.; Colon, Y. J.; Siu, P. W.; Scheidt, K. A.; Snurr, R. Q.; Hupp, J. T.; Farha, O. K. A facile synthesis of UiO-66, UiO-67 and their derivatives. *Chem. Commun.* **2013**, *49*, 9449-9451.

(19) Mendonca, M. L.; Ray, D.; Cramer, C. J.; Snurr, R. Q. Exploring the effects of node topology, connectivity, and metal identity on the binding of nerve agents and their hydrolysis products in metal-organic frameworks. *ACS Applied Materials & Interfaces* **2020**, *12* (31), 35657-35675.

(20) *Summary of the 2018 National Defense Strategy*. https://dod.defense.gov/Portals/1/Documents/pubs/2018-National-Defense-Strategy-Summary.pdf (accessed Dec 09, 2021).

(21) *U.S. Military Withdrawal and Taliban Takeover in Afghanistan: Frequently Asked Questions*. https://crsreports.congress.gov/product/pdf/R/R46879 (accessed Dec 09, 2021).

(22) *1925 Geneva Protocol*. https://www.un.org/disarmament/wmd/bio/1925-geneva-protocol/ (accessed Dec 09, 2021).

Appendix A: Glossary

Acetylcholine: A compound found in the synapse that must be broken down into acetic acid and choline by the enzyme acetylcholinesterase.

Adduct: The product of a reaction involving two or more reactants where the final product contains all atoms of the reactants.

Aqueous Buffer: A solution that contains a weak acid or base capable of resisting pH changes.

Azole: A five-membered ring that contains a nitrogen and at least one other atom that is not carbon (nitrogen, sulfur, etc.).

Catalytic Efficiency: How quickly a specific chemical reaction to take place with the help of a catalyst (which lowers the energy needed for the reaction to take place). An enzyme can perform this or another chemical.

Catalyze: Lowering the activation energy, or energy required for a reaction to take place. In effect this allows the reaction to take place more easily.

Chiral: A molecule that does not have a superimposable mirror image. Organic molecules can have multiple chiral atoms that have four differing substituents coming off the central atom. These compounds are optically active and can rotate plane polarized light.

Covalent: A chemical bond where the electrons are shared between two atoms of similar electronegativities.

Enzyme: A type of protein that catalyzes a biochemical reaction of interest.

Ester: A bond that has an oxygen connected to a carbon or phosphorus via a single bond. The same carbon or phosphorus is also connected to another oxygen via a double bond.

Hydrolysis: The use of water to break down a molecule into component parts.

Imidazole: An azole compound containing two nitrogen atoms in its five-membered ring.

Inorganic: A compound that does not contain carbon.

Isotherm: A line connecting points of equal temperature on a plot. An example could be a line connecting the same temperature for different pressures on a plot.

Kinetics: The study of the speed at which a chemical reaction takes place.

Lewis Acid: An atom or compound that is an electron acceptor in a chemical reaction. They are often used to catalyze organic chemistry reactions.

Lipophilic: Has an affinity for fats and can pass through them easily.

Mechanism: The step-by-step process of how a chemical reaction takes place, including reactants, changes in specific atoms, and compounds that leave during the reaction.

Mesoporous: A material that has pores with diameters between 2-50 nm.

Metal-Organic Framework: A crystalline structure containing inorganic nodes connected by organic linkers. These materials are porous in nature, highly adaptable, and can serve a multitude of uses.

Natural Fiber Welding: The process of using a molecular or ionic solvent to partially solubilize and reconstitute biopolymer fibers so they interact with one another and form a network that has different qualities than the native material.

Nerve Agents: A type of chemical warfare material that attacks the central nervous system.

Nuclear Magnetic Resonance Spectroscopy: A technique that analyzes the absorption of electromagnetic radiation in atomic nuclei by radio frequencies. This provides data on the type of atoms in a sample and their positioning in a molecule.

Organic: A compound containing carbon.

Organophosphate: Organic compounds containing a phosphorus atom that is part of an ester bond. These are common pesticides and nerve agents.

Simulant: An organophosphate with an altered functional group yielding it safe for laboratory use. Mimics actual organophosphates functionally.

Vapor Sorption Synthesis: A method of incorporating compounds into metal-organic frameworks that involves creating a vapor of the compound of interest and saturating the metal-organic framework with it.

$t_{1/2}$: The time required for half of the DMNP sample to be hydrolyzed.

Triazole: An azole containing three nitrogen atoms in the five-membered ring structure.

Volatile: A substance that is easily vaporized under ambient conditions. Often measured in units of mg m^{-3}.